



ELSEVIER

Solid State Ionics 135 (2000) 699–707

**SOLID
STATE
IONICS**

www.elsevier.com/locate/ssi

Measurement of ionic conductivity in mixed conducting compounds using solid electrolyte microcontacts

W. Zipprich^a, H.-D. Wiemhöfer^{b,*}^a*Inorganic Materials Research Laboratory, Department of Chemical Technology and MESA + Research Institute (CT1731), University of Twente, P.O. Box 217, 7500 AE Enschede, The Netherlands*^b*Institute for Inorganic Chemistry, University of Münster, Wilhelm-Klemm-Strasse 8, D-48149 Münster, Germany*

Abstract

Ion conducting (= electron blocking) microelectrodes were used to measure the oxygen ion conductivity in mixed conducting oxides as a function of the thermodynamic activity of oxygen. The reported data concern mixed conducting perovskites of the composition $\text{La}_{0.8}\text{E}_{0.2}\text{CoO}_3$ with $\text{E} = \text{Mg}, \text{Ca}, \text{Sr}$. The microelectrodes were made of yttrium-stabilized zirconia (radius 10–100 μm). Practical conditions and limitations of the microelectrode technique are described, e.g. the influence of the shape of the microelectrode, the microstructure of the interface and the pretreatment of the sample surface as well as further details for the measurement. Here, steady-state current–voltage curves were analyzed according to the Hebb–Wagner theory. The oxygen ion conductivity was calculated from these curves. The primary advantage of the microelectrode technique as compared to conventional planar contacts is the small effective diffusion length of about 10–100 μm due to the small electrode diameter and the radial geometry. Therefore, the time constants for approaching the steady state are two to four orders of magnitude lower as compared to a conventional thin sample with 1-mm thickness (= diffusion length). © 2000 Elsevier Science B.V. All rights reserved.

Keywords: Microelectrode; Ionic conductivity; Mixed conductor; Perovskites

Materials: $\text{La}_{1-x}\text{Sr}_x\text{CoO}_{3-\delta}$; $\text{La}_{1-x}\text{Ca}_x\text{CoO}_{3-\delta}$; $\text{La}_{0.8}\text{Mg}_{0.2}\text{CoO}_{3-\delta}$

1. Introduction

The basic concepts for the measurement of conductivities of minority charge carriers in mixed conductors were developed by Hebb [1], Wagner [2] and Yokota [3]. The main experimental techniques concern steady-state current–voltage curves or time-dependent polarization of the samples at (ion or

electron) blocking electrodes. Later on, Miyatani applied the same approach to the use of ion blocking platinum microcontacts which he called point contacts [4]. In the following, we use the term microcontact or microelectrode, because ‘point contacts’ have got a different meaning in physics. The technique was developed further and applied to various mixed conducting materials using ion as well as electron blocking microcontacts [5–8]. The latter are particularly useful for determining the ionic conductivity in the case of predominating electronic conduction (classical ‘electrode materials’). Mi-

*Corresponding author. Tel.: +49-251-833-3115; fax +49-251-833-8366.

E-mail address: hdw@uni-muenster.de (H.-D. Wiemhöfer).

crocontacts are particularly useful in the case of rather slow diffusion processes, because the diffusion length and therefore also the time to reach the steady state are reduced (by several orders of magnitude as compared to planar contacts on disc-shaped samples with about 1-mm thickness).

In this paper, we discuss the application of the microelectrode technique to the determination of the oxygen ion conductivity of mixed conducting oxides using stabilized zirconia as the electron blocking microcontact. Emphasis is laid on the experimental conditions and limitations of the microelectrode technique. As a model system, we have chosen the mixed conducting perovskites $\text{La}_{0.8}\text{E}_{0.2}\text{CoO}_{3-\delta}$ (E = Mg, Ca, Sr).

2. Cell geometry and theory

The electron blocking microelectrode material should exhibit a distinctly higher ionic conductivity than that of the mixed conducting specimen; otherwise, the additional impedance of the microelectrode (which usually has to be subtracted) lowers the accuracy. On the other hand, the electronic conductivity of the microelectrode material should be distinctly lower than the ionic conductivity of the specimen. If the latter condition fails, the microelectrode is no longer completely blocking for electrons as the electronic current through the microcontact will become of the order of the ionic current. The best choice was yttria-stabilized zirconia or the recently discovered oxygen ion conductor $\text{La}_{0.9}\text{Sr}_{0.1}\text{Gd}_{0.8}\text{Mg}_{0.2}\text{O}_{2.85}$ [9]. Both materials exhibit high oxygen ion conductivity and, in particular YSZ, low electronic conductivity. Doped ceria or doped bismuth oxides are much more limited in this respect because of their considerably higher electronic conduction, although their oxygen ion conductivity is higher. The electronic conductivity of doped ceria was recently determined by the use of ion blocking platinum microcontacts [8]. The latter is the ion blocking analogue to the electron blocking zirconia microcontact as used in this work.

As an extensive discussion of the theoretical background has been given elsewhere e.g. [5,6], only a brief summary will be given here of the equations

used for the evaluation of steady-state current–voltage curves at the microcontacts in terms of oxygen ion conductivities.

The assumed cell geometry consisted of a disc-shaped pellet contacted at the two opposite circular surfaces with an electron blocking YSZ microcontact and a large area planar contact (may be blocking or reversible) as illustrated in Fig. 1. The radius of the microcontact has to be small as compared to the thickness of the sample. The oxygen partial pressure $p_{\text{O}_2}^{\text{m.c.}}$ (m.c. stands for microcontact) in the mixed conductor directly at the microcontact is determined by the applied voltage according to the Nernst equation (high values of the partial pressure are to be understood as activities):

$$U = \frac{RT}{4F} \ln \frac{p_{\text{O}_2}^{\text{m.c.}}}{p_{\text{O}_2}} \quad (1)$$

For the samples, $\sigma_e \gg \sigma_{\text{O}_2}$ is assumed. Due to the higher electronic conductivity, a steady-state current in the mixed conducting oxides corresponds to a diffusion of oxygen in a local oxygen concentration gradient (= gradient of non-stoichiometry). The oxygen partial pressure difference throughout the specimen is determined in the steady state by the cell voltage U according to Eq. (1). Therefore, the local gradient is a definite function of the cell voltage, too (the local form of the gradient can be derived from Fick's law together with Eq. (1)). The largest part of the concentration gradient occurs near the microcontact as long as its contact radius is much smaller than the large area counter electrode.

$p_{\text{O}_2}^{\text{m.c.}}$ denotes the oxygen partial pressure in the surrounding gas phase and is assumed constant, because the current density near the planar contact is negligible. That part of the sample, therefore, remains in equilibrium with the surrounding constant oxygen partial pressure. Eq. (1) is valid under the following further assumptions: (a) the exchange of oxygen between the sample surface and the gas phase is negligible in the vicinity of the microcontact, (b) U must be the cell voltage along the zirconia electrolyte, i.e. between the microcontact and the air electrode at the top of the YSZ microelectrode in Fig. 1 (any further ohmic voltage drop in the sample or other parts of the cell has to be subtracted before

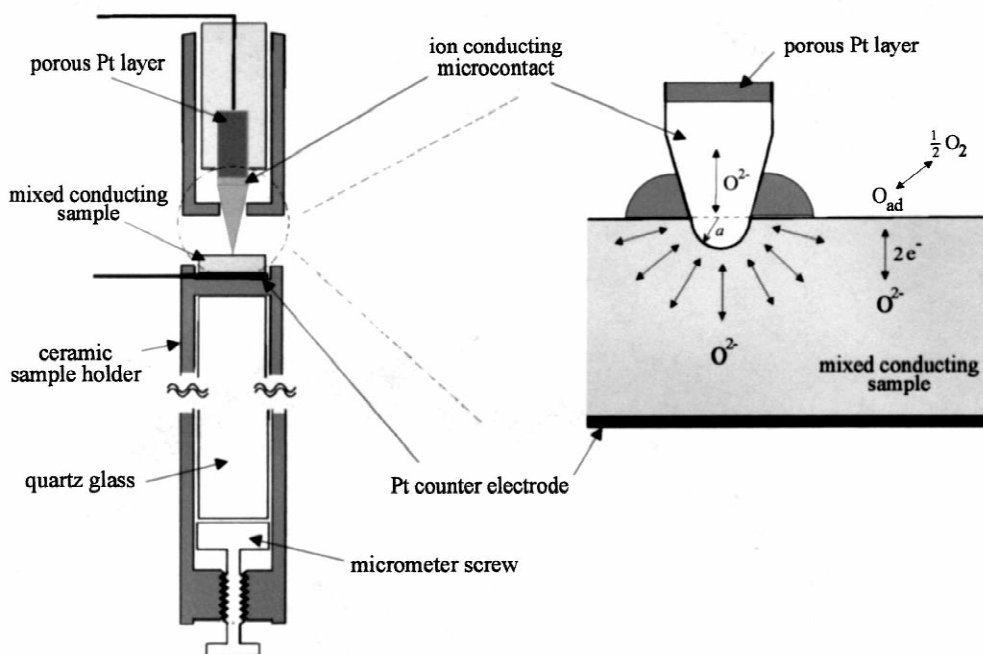


Fig. 1. (a) Experimental set-up, (b) electrochemical cell with ion-conducting microelectrode and encapsulation of the tip (schematic).

applying Eq. (1). To assure a negligible oxygen exchange with the gas phase the sample around the microcontact has to be encapsulated by glass or another insulating material.

Under these conditions, the Hebb–Wagner analysis can be applied which states that the ionic conductivity in the steady state is directly proportional to the slope of the current–voltage curve. Assuming a hemispherical geometry of the microcontact (with a as contact radius), one has [6]

$$\sigma_{\text{O}^{2-}}(p_{\text{O}_2}^{\text{m.c.}}) = \frac{1}{2\pi a} \cdot \frac{dI}{dU} \quad (2)$$

$\sigma_{\text{O}^{2-}}(p_{\text{O}_2}^{\text{m.c.}})$ is the local value of the ionic conductivity in the mixed conductor at the microcontact. It is clear that in the steady state there is normally a gradient of the ionic conductivity in the sample. Eq. (2) means that the slope of the current voltage curve gives full information on the functional dependence $\sigma_{\text{O}^{2-}}(p_{\text{O}_2}^{\text{m.c.}})$, because $p_{\text{O}_2}^{\text{m.c.}}$ can be calculated according to Eq. (1) from the given voltage U at the point where the slope dI/dU is taken in Eq. (2).

3. Experimental

The microelectrodes consisted of small rods made of yttrium-stabilized zirconia (10 mol% YSZ). The tip was formed to a hemispherical shape by careful polishing. The contact area was in the range $3 \cdot 10^{-4} \text{ mm}^2$ – $3 \cdot 10^{-2} \text{ mm}^2$ corresponding to a tip radius of 10–100 μm . Both, the sample surface and the tip of the microelectrode were polished with a 1- μm diamond paste just before the measurements to ensure a minimized roughness of the surface and to remove any reaction layers or passivating films. The backside of the microelectrode, opposite to the sample contact, was covered by a porous sintered platinum layer and contacted to a Pt wire.

The perovskite samples were flat pellets with diameters of 5–10 mm and a height of 1–2 mm. Details of the preparation of the perovskite samples have been given in a previous publication [7]. The relative densities of the samples were in the range of 94–96% of the theoretical density. The backside of the pellets was contacted to a Pt foil that acted as the counter electrode vs. the microcontact.

The set-up with oven and electrochemical cell was mounted vertically as shown in Fig. 1; the sample holder and the outer tube were made of aluminum oxide and quartz glass, respectively. The microelectrode was movable in the vertical direction; the contact pressure was regulated by a load on the microelectrode holder. A well reproducible contact with constant contact pressure was achieved in this way. The cell was electrically shielded and placed in an oven. The temperature was held constant (PID control).

Current–voltage curves were measured in a temperature range between 550°C and 750°C by applying a triangular voltage ramp to the sample starting at 0 mV to +150 mV, going from +150 mV to –150 mV and back from –150 mV to 0 mV again (potentiostat: Jaissle 1002 T-NC). The resulting currents were in the range of few nA to some hundred nA depending on the ionic conductivity of the sample. The current was measured for voltage intervals of 5 mV, the voltage scan rate was in the range of 0.5 to 1 mV/s. To determine appropriate scan rates, experiments were carried out to examine the reproducibility and hysteresis of the current–voltage curves at different voltage scan rates. Measurements were carried out, if the remaining potential was 0 mV (± 1 mV) during a period of at least 1 h.

The contribution of additional ohmic voltage drops in the cell was checked by switching off the external voltage and monitoring the time dependence of the cell voltage decay. In practically all experiments, the ohmic voltage drop was very small. This also implies that thermodynamic equilibrium is attained at the interface of the sample and the microelectrode under charge flow during the measurement, because the cell voltage directly after switching off the external voltage source (i.e. with zero current) has the same value as before.

4. Discussion of methodic aspects

The accuracy of the oxygen ion conductivity as determined from Eq. (2) depends on the accuracy of the radius a of the microcontact and of the current voltage curve itself. Therefore, the contact area

between sample and microcontact has to be measured as precisely as possible. After removing the YSZ tip, the area of the microcontact was detectable under an optical microscope on the sample surface as a small hole (due to the greater hardness of the YSZ). Therefore, the contact radius was usually determined under the microscope. The error of the as-determined radius is about 5–20%. It represents an effective constant, because the real contact surface deviates more or less from an exact half sphere due to different penetration depths of the tip.

Some limitations for the applicability of the method depend on the material that is chosen for the microelectrode. The resistance of the sample as well as that of the microelectrode can be viewed as consisting of the two parallel resistances of electrons and ions. First, the ionic conductivity of the sample to be measured should be lower than the ionic conductivity of the microelectrode (=upper limit). Otherwise, the accuracy tends to become low. To improve the accuracy, normally a correction for the ohmic drop in the microelectrode (and, perhaps, in other parts of the cell) should be made. The series resistance of a typical YSZ microelectrode ($a=50$ μm) in the cell was 9 k Ω at 750°C and 12 k Ω at 700°C. Only samples with an ionic conductivity of more than 10^{-3} ($\Omega\text{ cm}$) $^{-1}$ have ionic resistances of the order of 10 k Ω . On the other hand, also a lower limit of the measurable ionic conductivity occurs due to the small, but finite electronic conductivity of the zirconia microelectrode. The ionic conductivity of the sample material should be higher than the electronic conductivity of the microelectrode material. Otherwise, a non-negligible electronic current will flow through the microcontact in parallel to the ionic one, because then an ideal blocking of electrons is not possible. In the case of YSZ as the microelectrode material, the condition $\sigma_{\text{O}^{2-}}(\text{sample}) \gg \sigma_{\text{e}}(\text{YSZ})$ is very well fulfilled down to oxygen conductivities of 10^{-8} ($\Omega\text{ cm}$) $^{-1}$ at 700°C.

The decay and geometry of the concentration gradients were simulated by solving Fick's law according to the method of finite differences for hemispherical and circular contact area and a pellet (i.e. cylindrical sample). The result was that — provided the contact radius is small compared to the distance to the counter electrode — in a large range

around the microcontact, the hemispherical geometry of current lines and isoconcentration surfaces is a very good approximation.

The evaluation of the experiments in terms of conductivities relies on the achievement of a steady state. This is a very important condition. In all our measurements, the ratio between the thickness d of the sample pellets and the contact radius a was in the range $d/a=20\text{--}200$. Optimal values would be $d/a > 100$. However, problems arise with samples that show low ionic conductivities as then a small contact radius leads to very low current levels that are difficult to measure.

The typical time constant to reach the steady state for a semi-infinite hemispherical diffusion geometry is ideally given by $\tau = a^2/2D$ with D as the chemical diffusion coefficient of oxygen in the mixed conducting oxide sample. Results of simulations show, however, that the time for attaining reproducible steady state conditions will become considerably longer (at least 10τ), if a non-ideal geometry with $d/a < 20$ is used. In those cases, hysteresis will be observed in the current voltage curves due to the non-negligible influence of the concentration gradient near the planar counter electrode that adds a slow background relaxation to the time dependence with long time constant. Observation of hysteresis thus indicates that the planar counter electrode geometry cannot be neglected as we do in our ideal spherical approximation of the contact geometry (which is the basis for Eq. (2)).

Another crucial effect which has to be excluded in any case is an oxygen exchange between the gas phase and the sample surface around the microcontact. It may arise (a) from a fast electrode reaction with gaseous oxygen at the interface between sample and microcontact which adds an electronic current and thus leads to higher current values, or (b) from a fast exchange kinetics of oxygen at the free sample surface which hinders the formation of radial concentration gradients near the microcontact. Case (a) is favored by a high surface roughness, which leads to additional gas-filled channels and cavities at the interface of the microelectrode. Case (b) can be prevented by covering the surface with a dense insulating layer (normally a glass). A further critical point is a high porosity of the mixed conductor (e.g.

at densities considerably lower than 95% of the theoretical density), because a considerable amount of oxygen pore diffusion apparently accelerates the diffusion and leads to erroneously high ionic conductivity values. This is a critical factor in all electrochemical techniques that analyze oxygen ion transport in mixed conductors as discussed recently by Sunde et al. [10].

Examples for current voltage curves of a $\text{La}_{0.8}\text{Sr}_{0.2}\text{CoO}_{3-\delta}$ sample with and without a polished surface are shown in Fig. 2. Significant differences are found between curves of a carefully polished sample and a sample with an unpolished surface. However, in the case of lanthanum cobaltites, part of this effect is due to passivating surface layers that already are detectable after a one-day storage of such samples in air. A thick passivating layer leads to an increased cell resistance and normally to a linear current–voltage curve with large ohmic drop. The deviations of curve I_1 from I_2 in Fig. 2 for higher positive voltages (=high oxygen partial pressures) are clearly due to exchange of oxygen with the gas phase at the interface of the microcontact ('electrode reaction').

If the samples have no extended pores and if an encapsulation of the sample surface around the microelectrode is possible, this is the best way to eliminate gas exchange. Fig. 3 compares current voltage curves of a polished sample with and without

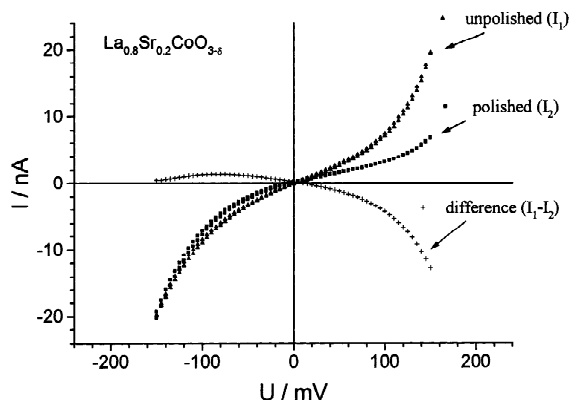


Fig. 2. Current–voltage curves of a YSZ microcontact on a $\text{La}_{0.8}\text{Sr}_{0.2}\text{CoO}_{3-\delta}$ sample (a) polished surface, (b) unpolished surface (600°C , $a=100\ \mu\text{m}$). Only small hysteresis was found measuring forward and back.

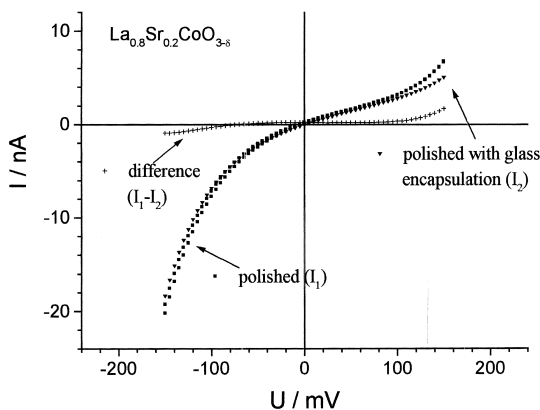


Fig. 3. Current–voltage curves of a $\text{La}_{0.8}\text{Sr}_{0.2}\text{CoO}_{3-\delta}$ sample (a) with glass encapsulation, (b) without encapsulation around the microelectrode (600°C , $a=100\ \mu\text{m}$). Only small hysteresis was found measuring forward and back.

encapsulation of the microelectrode. Except for the encapsulation of the microelectrode, the conditions were the same as in Fig. 2. It is evident that the two curves are nearly coinciding except at high positive voltages (high oxygen partial pressures).

For $\text{La}_{0.8}\text{Sr}_{0.2}\text{CoO}_{3-\delta}$, the result in Fig. 3 shows that, after careful surface polishing, the electrode reaction at the circumference of the microcontact is negligible for low voltages which indicates a slow surface exchange reaction at the applied temperatures. This demonstrates that the method can also be used to yield further information on the kinetics of surface exchange reactions.

5. Results on some oxides

In Figs. 4–6, we present examples of results of measurements with the microelectrode technique on lanthanum cobaltites doped with the earth alkaline elements Mg, Ca and Sr. Fig. 4 shows results on Ca- and Sr-doped samples for two different dopant concentrations at 700°C . At least for lower dopant concentrations, the oxygen ion conductivity increases towards low oxygen partial pressures as is expected for a vacancy transport. The increase in the opposite direction at high oxygen partial pressures for the two $x=0.2$ curves may be due to formation of gaseous

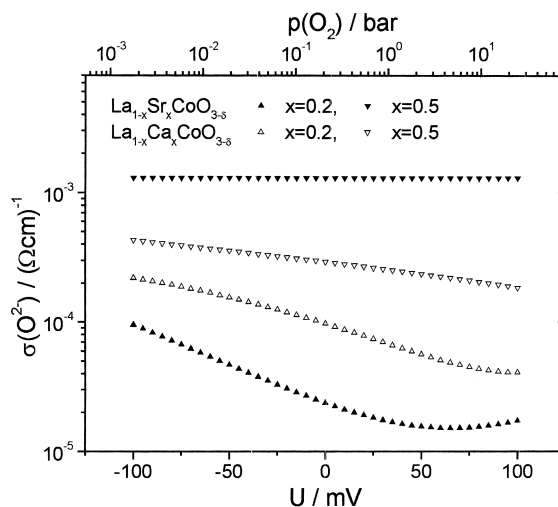


Fig. 4. Ionic conductivities of Sr- and Ca-doped cobaltites $\text{La}_{1-x}\text{E}_x\text{CoO}_{3-\delta}$ with $\text{E}=\text{Ca}, \text{Sr}$ and $x=0.2, 0.5$ at 700°C from steady-state current voltage curves at YSZ microelectrodes (radius was 40 and 50 μm).

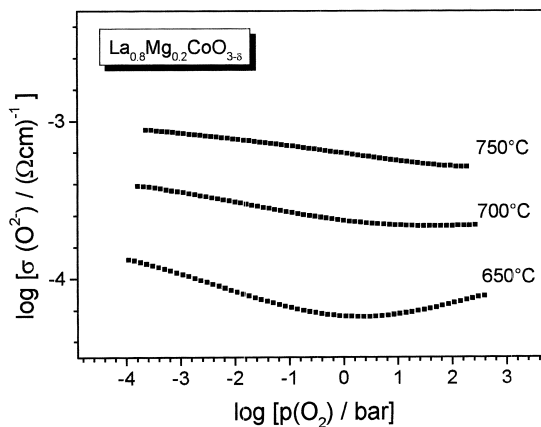


Fig. 5. Ionic conductivities of a cobaltite sample with the nominal composition $\text{La}_{0.8}\text{Mg}_{0.2}\text{CoO}_{3-\delta}$ from steady-state current voltage curves at YSZ microelectrodes (radius was 40 μm).

oxygen (electrode reaction) which is inevitable at these high oxygen pressures.

Table 1 compares selected conductivity values for perovskites $\text{La}_{1-x}\text{Sr}_x\text{CoO}_{3-\delta}$ and silver with values published by other authors. Table 2 gives a more detailed comparison of oxygen ion conductivity

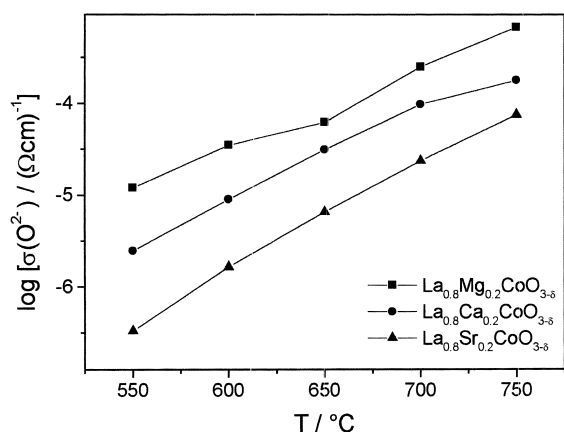


Fig. 6. Comparison of ionic conductivities in air of the three cobaltite materials as a function of temperature.

Table 1

Comparison of measured oxygen ion conductivities as measured by the microelectrode technique (YSZ contacts) with literature data

Sample	T (°C)	$\sigma_{\text{O}^{2-}}$ (Ω cm) ⁻¹ This work	$\sigma_{\text{O}^{2-}}$ (Ω cm) ⁻¹ Literature
La _{0.4} Sr _{0.6} CoO _{3-δ}	700	6.3 · 10 ⁻⁴	7.6 · 10 ⁻³ [15]
La _{0.5} Sr _{0.5} CoO _{3-δ}	700	1.3 · 10 ⁻³	1.8 · 10 ⁻² [15]
Ag	600	3.2 · 10 ⁻⁴	2.5 · 10 ⁻⁴ [16]
Ag	700	1.3 · 10 ⁻³	1.0 · 10 ⁻³ [17]

values for the often-investigated La_{0.8}Sr_{0.2}CoO_{3-δ}. The literature values are obtained by techniques such as measurement of oxygen permeation and con-

centration relaxation after a stepwise change of gaseous oxygen pressure. In most cases, data were available to calculate or estimate the oxygen ion conductivity from the published data.

It is evident from Table 2 that much larger values for diffusion coefficient and ionic conductivity are found in samples with low ($\leq 90\%$ of theory) density. The investigations with dense samples ($\geq 95\%$) yielded much lower values. Our experience with the microelectrode technique (as well as the discussion of the various disturbing influences above) showed that in most cases the measured conductivities tend to be considerably higher, if lower sample densities or rough interfaces were present. Accordingly, the density of the mixed conducting oxide samples will definitely play a decisive role for the accuracy of the measurement.

Further examples can be found in the literature with much larger differences for the diffusion coefficients of La_{1-x}Sr_xCoO_{3-δ} than reported in Table 2 [11,12] (differences up to a factor of 10⁶), even for tracer diffusion coefficients of different authors as measured by the same method [13–19]. In all these cases, porosity, especially interconnected porosity is the most important cause for spuriously high diffusion coefficients [12]. Routbart et al. [11] also argue that these discrepancies arise due to additional diffusion paths depending on the sample preparation and acting as short circuit paths, e.g. grain boundary diffusion, gas phase or surface diffusion in pores.

Extrapolating the values of the ionic conductivity of La_{0.8}Sr_{0.2}CoO_{3-δ} determined in our study to 1000°C gives a value of 5 · 10⁻³ (Ω cm)⁻¹, a value

Table 2

Values for the oxygen ion conductivity of La_{0.8}Sr_{0.2}CoO_{3-δ} and relative densities of the samples as derived from various references: the listed values were directly taken from the references or calculated using the available data

$\sigma_{\text{O}^{2-}}$ (Ω cm) ⁻¹	T (°C)	Rel. density (%)	Method ^a	Reference
2.4 · 10 ⁻⁵	700	~95	mc	This work
2.0 · 10 ⁻⁴	700	93–99	p	[18]
4.0 · 10 ⁻³	700	>90	SIMS	[19]
3.0 · 10 ⁻¹	830	85	p	[20]
8.3 · 10 ⁻³	900	–	tg	[21]
5.0 · 10 ⁻³	1000	~95	mc	This work ^b
3.7 · 10 ⁻³	1000	93–99	p	[22]

^a Techniques: mc — microcontact, tg — thermogravimetry, p — permeation, SIMS — tracer diffusion/SIMS.

^b Extrapolated value.

that corresponds well with the value of van Doorn ($3.7 \cdot 10^{-3} (\Omega \text{ cm})^{-1}$) calculated from diffusion coefficients that were determined by permeation experiments at very dense samples (relative density 93–99%, see Table 2).

Our values for the ionic conductivities are about the lowest. However, as experimental influences and possible errors in the microelectrode technique tend to increase the measured values (see discussion above), we assume that the lower ionic conductivities are more realistic.

In Table 1, values for effective oxygen conductivities in bulk silver are also given. Silver has solubility for oxygen at elevated temperatures. The oxygen ion conductivity given in Table 1 for silver is an effective value under the assumption that only oxygen ions are exchanged at the interface to the YSZ microcontact. An analysis of the measurement with electron blocking electrode on silver by C. Wagner's concepts of irreversible thermodynamics as described earlier in Ref. [14] shows that neutral oxygen transport can be analyzed as a coupled co-transport of oxygen ions and electrons and is described by an effective oxygen ion conductivity. The as-derived conductivities are in good agreement with literature values.

Fig. 5 shows values for the oxygen ion conductivity of a Mg-doped sample with the nominal composition $\text{La}_{0.8}\text{Mg}_{0.2}\text{CoO}_{3-\delta}$. Mg is expected to occupy B-sites contrary to Ca and Sr. Therefore, the above composition will lead to a La deficit and/or an additional CoO phase. Surprisingly as the comparison in Fig. 6 shows, the sample material exhibits higher ionic conductivity in air as compared to the Ca- or Sr-doped cobaltite systems. The interpretation, however, is not straightforward. In the $\text{La}_{0.8}\text{Mg}_{0.2}\text{CoO}_{3-\delta}$ sample, only a small amount of CoO was detected besides a predominant perovskite phase. The X-ray powder diffraction pattern could well be fitted by that of a rhombohedral perovskite cell with a high La deficit on the A-site. If the amount of Co precipitated as CoO is considered negligible and Mg occupies B-sites, then the stoichiometric composition should be approximately described by $\text{La}_{0.67}[\text{Mg}_{0.17}\text{Co}_{0.83}]\text{O}_{2.42}$, where the brackets incorporate the B-sites. The latter is equivalent to a high deficit on La and oxygen ion sites that can explain the relatively high oxygen ion conductivity.

6. Conclusions

The microelectrode technique for the determination of oxygen ion conductivity in mixed conducting oxides is described in this work. Experiences, experimental details and important limitations of this method are also given.

The results for $\text{La}_{0.8}\text{Sr}_{0.2}\text{CoO}_{3-\delta}$, demonstrate the crucial role of sample porosity in producing large deviations of the measured conductivities due to gaseous pore diffusion of oxygen which short-circuits the much slower bulk diffusion.

A surprising result was that the sample with nominal composition $\text{La}_{0.8}\text{Mg}_{0.2}\text{CoO}_{3-\delta}$ shows a higher oxygen ion conductivity than samples with Ca or Sr substitution. As the small Mg^{2+} ions will occupy Co^{3+} positions in the lattice, a more appropriate formula is $\text{La}_{0.67}[\text{Mg}_{0.17}\text{Co}_{0.83}]\text{O}_{2.42}$ which implies a high oxygen vacancy concentration due to a high metal deficit on the A sites of the ABO_3 structure.

Acknowledgements

We are grateful to the DFG and the FCI for financial support of this work which was carried out as part of a DFG project at the University of Münster.

References

- [1] M.H. Hebb, J. Chem. Phys. 20 (1952) 185.
- [2] C. Wagner, Proceedings of the Seventh Meeting of the International Commission on Electrochemical, Thermodynamics and Kinetics, Butterworths, London, 1957.
- [3] I. Yokota, J. Phys. Soc. Jpn. 16 (1961) 2213.
- [4] S. Miyatani, J. Phys. Soc. Japan 11 (1956) 1059.
- [5] H. Rickert, H.-D. Wiemhöfer, Solid State Ionics 11 (1983) 257.
- [6] H.-D. Wiemhöfer, Ber. Bunsenges. Phys. Chem. 97 (3) (1993) 461.
- [7] W. Zipprich, S. Waschilewski, F. Rocholl, H.-D. Wiemhöfer, Solid State Ionics 101–103 (1997) 1015.
- [8] S. Lübke, H.-D. Wiemhöfer, Solid State Ionics 117 (1999) 229–243.
- [9] M. Feng, J.B. Goodenough, Eur. J. Solid State Inorg. Chem. 31 (1994) 663.
- [10] S. Sunde, K. Nisancioglu, T. Gür, J. Electrochem. Soc. 143 (11) (1996) 3497.

- [11] J.L. Routbart, R. Doshi, M. Krumpelt, *Solid State Ionics* 90 (1996) 21.
- [12] R. Doshi, J. Routbart, C. Alcock, *Defect and Diffusion Forum* 127–128 (1995) 39.
- [13] T. Ishigaki, S. Yamauchi, K. Kishio, J. Mizusaki, K. Fueki, *J. Solid State Chem.* 73 (1988) 179.
- [14] H.-D. Wiemhöfer, *Solid State Ionics* 40–41 (1990) 530.
- [15] N. Itoh, T. Kato, K. Uchida, K. Haraya, *J. Membr. Sci.* 92 (1994) 239.
- [16] I. Kontoulis, B.C.H. Steele, *Solid State Ionics* 47 (1991) 317.
- [17] T.A. Ramanarayanan, R. Rapp, *Metallurg. Trans.* 3 (1972) 3239.
- [18] M.H.R. Lankhorst, Thesis, University of Enschede, Netherlands, 1997.
- [19] S. Carter, A. Selcuk, J. Chater, R. Kajda, J. Kilner, B.C.H. Steele, *Solid State Ionics* 53–56 (1992) 597–605.
- [20] V.V. Kharton, E. Maumovich, A.A. Vecher, A. Nikolaev, *J. Solid State Chem.* 120 (1995) 128–136.
- [21] S. Sekido, H. Tachibani, Y. Yamamura, T. Kambara, *Solid State Ionics* 37 (1990) 253–259.
- [22] R.H.E. van Doorn, Thesis, University of Enschede, Netherlands, 1996.